ARTICLE

Exons as units of phenotypic impact for truncating mutations in autism

Andrew H. Chiang[1,2] · Jonathan Chang[1,2] · Jiayao Wang[1,2] · Dennis Vitkup [1,2]

Abstract

Autism spectrum disorders (ASD) are a group of related neurodevelopmental diseases displaying significant genetic and phenotypic heterogeneity. Despite recent progress in understanding ASD genetics, the nature of phenotypic heterogeneity across probands remains unclear. Notably, likely gene-disrupting (LGD) de novo mutations affecting the same gene often result in substantially different ASD phenotypes. Nevertheless, we find that truncating mutations affecting the same exon frequently lead to strikingly similar intellectual phenotypes in unrelated ASD probands. Analogous patterns are observed for two independent proband cohorts and several other important ASD-associated phenotypes. We find that exons biased toward prenatal and postnatal expression preferentially contribute to ASD cases with lower and higher IQ phenotypes, respectively. These results suggest that exons, rather than genes, often represent a unit of effective phenotypic impact for truncating mutations in autism. The observed phenotypic patterns are likely mediated by nonsense-mediated decay (NMD) of splicing isoforms, with autism phenotypes usually triggered by relatively mild (15–30%) decreases in overall gene dosage. We find that each ASD gene with recurrent mutations can be characterized by a parameter, phenotype dosage sensitivity (PDS), which quantifies the relationship between changes in a gene's dosage and changes in a given disease phenotype. We further demonstrate analogous relationships between exon LGDs and gene expression changes in multiple human tissues. Therefore, similar phenotypic patterns may be also observed in other human genetic disorders.

Introduction

Recent advances in neuropsychiatric genetics [1–4] and, specifically, in the study of autism spectrum disorders (ASD) [5–8] have led to the identification of multiple genes and specific cellular processes that are affected in these diseases [5, 6, 8–10]. However, phenotypes associated with

✉ Dennis Vitkup
   dv2121@columbia.edu

[1] Department of Biomedical Informatics, Columbia University, New York, NY, USA

[2] Department of Systems Biology, Center for Computational Biology and Bioinformatics, Columbia University, New York, NY, USA

ASD vary considerably across autism probands [11–14], and the nature of this phenotypic heterogeneity is not well understood [15, 16]. Despite the complex genetic architecture of ASD [17–22], a subset of cases from simplex families, i.e. families with only a single affected child among siblings, are known to be strongly affected by de novo mutations with severe deleterious effects [8, 23, 24]. Interestingly, despite their less complex genetic architecture, simplex autism cases often display as much phenotypic heterogeneity as more general ASD cohorts [25–27]. This provides an opportunity for an in-depth exploration of the etiology of the autism phenotypic heterogeneity using accumulated phenotypic and genetic data. In this study we performed such an analysis, focusing on severely damaging, so-called likely gene-disrupting (LGD) mutations, which include nonsense, splice site, and frameshift variants. We explored genetic and phenotypic data collected in the Simons Simplex Collection (SSC) [28] and then validated our results using an independent ASD cohort from the Simons Variation in Individuals Project (VIP) [29].

We investigated in the paper the effects of LGD mutations on cognitive and other important ASD-related

phenotypes, including adaptive behavior, motor skills, communication, and coordination. These analyses allowed us to understand how the exon–intron structure of human genes contributes to observed phenotypic heterogeneity. We next explored the quantitative relationships between changes in gene dosage induced by nonsense-mediated decay (NMD) and the phenotypic effects of LGD mutations. To that end, we introduced a new genetic parameter, which quantifies how changes in a gene's dosage affect specific autism phenotypes. Finally, we described how simple linear models of gene dosage can explain a substantial fraction of the phenotypic heterogeneity in the analyzed simplex ASD cohorts.

Results

We first considered the impact of de novo LGD mutations on several well-studied cognitive phenotypes: full-scale (FSIQ), nonverbal (NVIQ), and verbal (VIQ) intelligence quotients [5, 8, 10]; these scores are normalized by age and standardized across a broad range of phenotypes [28]. We analyzed de novo mutations and the corresponding phenotypes of ASD probands for more than 2500 families from SSC [28]. Notably, we found that the average IQ differences between probands with LGD mutations in the same gene were only slightly smaller than the IQ differences between all pairs of probands; the mean pairwise IQ difference for probands with mutations in the same gene was 25.7 NVIQ points, while the mean difference for all pairs of probands was 29.4 NVIQ points (~12% difference, Mann–Whitney U one-tail test $p = 0.14$; Supplementary Table 1).

We next asked whether probands with LGD mutations at similar locations within the same gene resulted, on average, in more similar phenotypes (Supplementary Fig. 1). Indeed, IQ differences between probands with LGD mutations closer than 1000 base pairs apart were significantly smaller than the IQ differences between probands with more distant mutations; NVIQ average difference of 10.4 points for ≤1000 bp, NVIQ average difference of 28.6 points for >1000 bp (MWU one-tail test $p = 0.005$). However, across the entire range of nucleotide distances between LGD mutations in the same genes, we did not observe either a significant correlation or a monotonic relationship between IQ differences and mutation proximity (NVIQ Spearman's $\rho = 0.1$, $p = 0.4$; Mann–Kendall one-tail trend test $p = 0.5$).

To explain the observed patterns of phenotypic similarity, we next considered the exon–intron structure of target genes. Specifically, we investigated phenotypes resulting from truncating mutations affecting the same exon in unrelated ASD probands. In this analysis, we took into account LGD mutations in the exon's coding sequence as
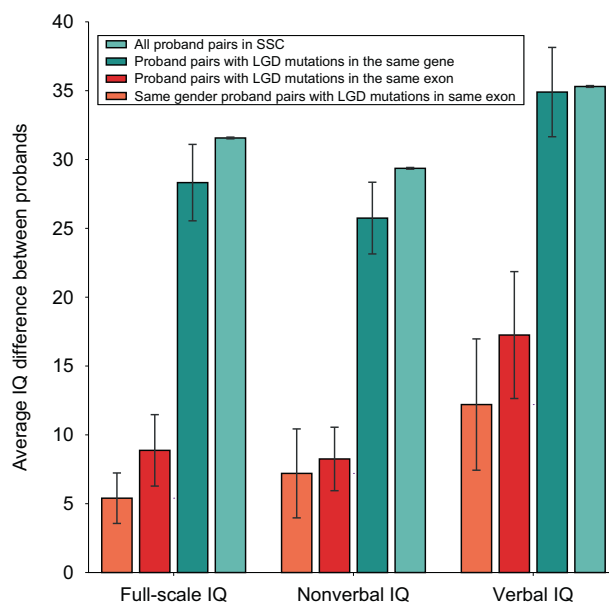

Fig. 1 Average difference in IQ scores between SSC probands. From left to right, the sets of bars represent probands' differences in full-scale, nonverbal, and verbal IQs. Within each bar set, from right to left, the bars represent the average IQ difference between pairs of probands in the entire SSC cohort (light green), between proband pairs with de novo LGD mutations in the same gene (dark green), between proband pairs with de novo LGD mutations in the same exon (red), and between proband pairs of the same gender and with de novo LGD mutations in the same exon (orange). Error bars represent the SEM.

well as disruptions of the exon's flanking canonical splice sites, since such splice site mutations should affect the same transcript isoforms (Supplementary Fig. 2). The analysis of 16 unrelated ASD probands (8 pairs with LGD mutations in the same exons) showed that they have strikingly more similar phenotypes (Fig. 1, red bars) compared to probands with LGD mutations in the same gene (Fig. 1, dark green bars); same exon FSIQ/NVIQ/VIQ average IQ difference 8.9, 8.3, 17.3 points, same gene average difference 28.3, 25.7, 34.9 points (Mann–Whitney U one-tail test $p = 0.003$, 0.005, 0.016). Because of well-known gender differences in autism susceptibility [5, 30, 31], we also compared IQ differences between probands of the same gender harboring truncating mutations in the same exon (Fig. 1, orange bars) to IQ differences between probands of different genders; same gender FSIQ/NVIQ/VIQ average difference 5.4, 7.2, 12.2; different gender average difference 14.7, 10, 25.7 (MWU one-tail test $p = 0.04$, 0.29, 0.07). Thus, stratification by gender further decreased the observed phenotypic differences between probands with LGD mutations in the same exon. Notably, the patterns of phenotypic similarity between different probands only extended to mutations affecting the same exon. The average IQ differences between probands with LGD mutations in neighboring exons were not significantly different compared to mutations in non-neighboring exons (MWU one-tail test $p = 0.6$,
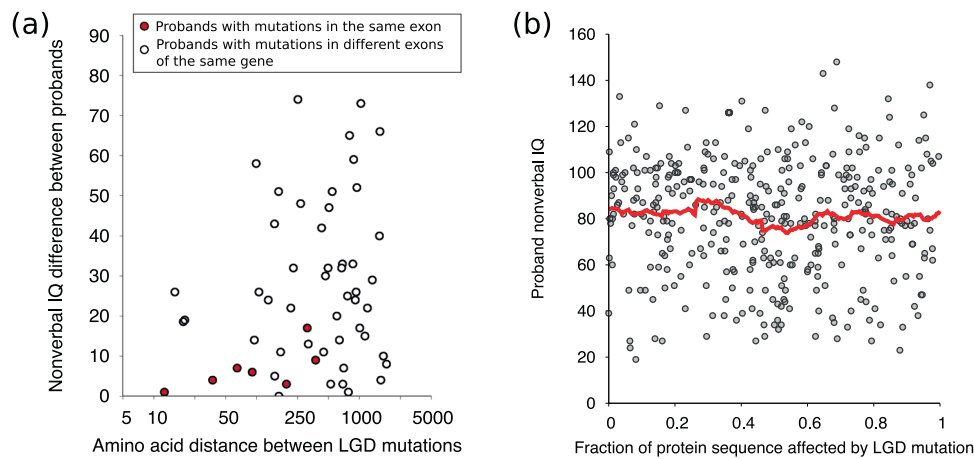
Fig. 2 The relationship between the position of de novo LGD mutations in protein sequence and probands' IQ scores. a Amino acid distance between LGD mutations in protein sequence versus differences in nonverbal IQ (NVIQ). Each point corresponds to a pair of probands with LGD mutations in the same gene. The *x*-axis represents the amino acid distance between protein sites of LGD mutations, and the *y*-axis represents the difference between the corresponding probands' NVIQs. Red points represent pairs of probands with LGD mutations in the same exon, and white points represent pairs of probands with mutations in the same gene but different exons. **b** Relative fraction of protein sequence truncated by LGD mutations versus corresponding probands' NVIQs. Each point corresponds to a single proband affected by an LGD mutation. The *x*-axis represents the fraction of protein sequence (i.e. fraction from the first amino acid) truncated by the mutation, and the *y*-axis represents the corresponding proband's NVIQ. The red line represents the moving average of the data calculated using an interval of width 0.05.

0.18, 0.8; Supplementary Fig. 3). The observed effects were also specific to LGD mutations, i.e. probands with either synonymous ($p = 0.93, 0.97, 0.95$; Supplementary Fig. 4) or missense ($p = 0.8, 0.5, 0.8$; Supplementary Fig. 5) mutations in the same exon were as phenotypically diverse as random pairs of ASD probands.

We next explored the relationship between phenotypic similarity and the proximity of truncating mutations in the corresponding protein sequences. This analysis revealed that probands with LGD mutations in the same exon often had similar IQs, despite being affected by truncating mutations separated by scores to hundreds of amino acids in protein sequence (Fig. 2a and Supplementary Fig. 6). Furthermore, we found probands with LGD mutations in the same exon to be more phenotypically similar than probands with LGD mutations separated by comparable amino acid distances in the same protein sequence but not necessarily in the same exon (NVIQ distance-matched permutation test $p = 0.002$; Supplementary Fig. 7). We then investigated whether de novo mutations truncating a larger fraction of protein sequences resulted, on average, in more severe intellectual phenotypes. Surprisingly, this analysis showed no significant correlations between the fraction of truncated protein and the severity of the resulting intellectual phenotypes (Fig. 2b); NVIQ Pearson's $R = 0.05$ ($p = 0.35$; Supplementary Fig. 8). We also did not find any significant biases in the distribution of truncating de novo mutations across protein sequences compared with the distribution of synonymous de novo mutations (Kolmogorov–Smirnov two-tail test $p = 0.9$; Supplementary Fig. 9). It is possible

that the lack of correlation between phenotypic impact and the fraction of truncated sequence is due to the averaging of phenotypic effects across different proteins. Therefore, for genes with recurrent mutations, we used a paired test to investigate whether truncating a larger fraction of the same protein sequence led to more severe phenotypes. This analysis showed no substantial phenotypic difference due to LGD mutations truncating different fractions of the same protein (average NVIQ difference 0.24 points; Wilcoxon signed-ranked one-tail test $p = 0.44$). We also investigated, using the Pfam database [32], whether mutations that truncate the same protein domain led to smaller phenotypic differences. The results demonstrated that mutations in different exons, even when truncating the same protein domain, resulted in phenotypes as different as due to LGD mutations in the same protein (average NVIQ differences = 28.1; Supplementary Fig. 10).

The results presented above suggest that it is the occurrence of de novo LGD mutations in the same exon, rather than simply the proximity of mutation sites in protein or nucleotide sequences, that is primarily responsible for the similar phenotypic consequences observed in unrelated probands. To explain this result, we hypothesized that truncating mutations in the same exon usually affect, due to nonsense-mediated decay (NMD) [33], the expression of exactly the same sets of splicing isoforms. Therefore, such mutations should lead to particularly similar phenotypes, both through similar decreases in overall gene dosage and similar perturbations to the mRNA expression of affected transcriptional isoforms. To test this mechanistic model, we
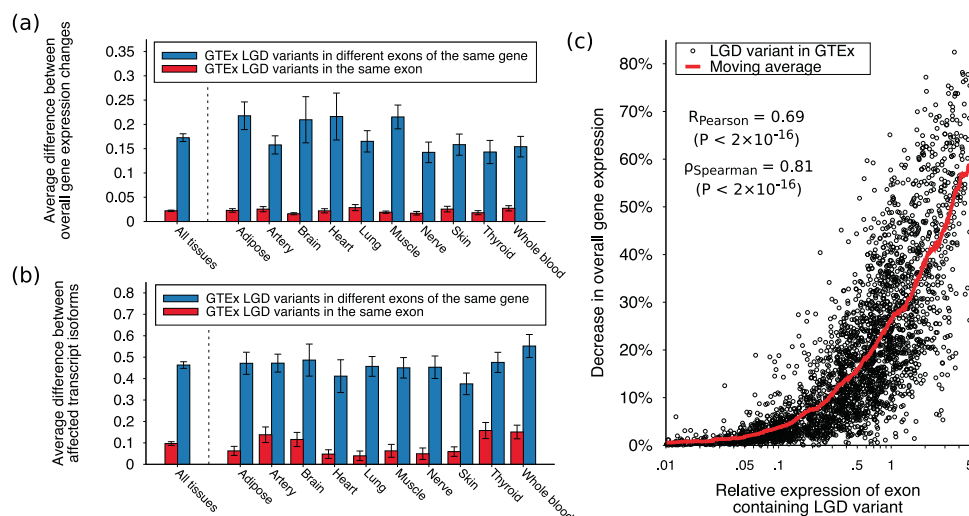
Fig. 3 Gene expression changes across human tissues induced by LGD variants in the same exon and in the same gene but in different exons. Expression changes (decreases) induced by LGD variants were calculated based on data from the Genotype and Tissue Expression (GTEx) Consortium [34]. **a** Bars represent the average differences between pairs of individuals from the GTEx cohort in overall gene expression changes induced by distinct LGD variants in the same exon (red) and in the same gene but in different exons (blue). Error bars represent the SEM. **b** Bars represent the average differences between pairs of individuals from the GTEx cohort in isoform-specific expression changes induced by distinct LGD variants in the same exon (red) and in the same gene but in different exons (blue). Differences in expression changes across transcriptional isoforms were quantified using the angular distance metric between vectors representing isoform-specific expression changes (see Methods). Error bars represent the SEM. **c** Relationship between the relative expression of exons harboring LGD variants in GTEx and the corresponding NMD-induced decreases in overall gene expression. Each point corresponds to an LGD variant in one of ten human tissues. The x-axis represents the relative expression of an exon harboring an LGD variant in a tissue; the relative expression of an exon was calculated as the ratio between the exon expression level and the overall expression level of the corresponding gene (see Methods). The y-axis represents the NMD-induced decrease in overall gene expression (see Methods). Red line represents the moving average of the data calculated using an interval of width 0.1 (log-scaled).

used data from the Genotype and Tissue Expression (GTEx) Consortium [34, 35], which collected exome sequencing and corresponding human tissue-specific gene expression data from hundreds of individuals and across multiple tissues. Using ~4400 LGD variants in coding regions and corresponding RNA-seq data, we compared the expression changes resulting from LGD variants in the same exon and different exons of the same gene (Fig. 3a, b). Specifically, for each truncating variant, we analyzed allele-specific read counts [36] and then used an empirical Bayes approach to infer the effects of NMD on gene expression (see Methods). This analysis confirmed that the gene dosage changes for individuals with LGD variants in the same exon were, on average, ~7 times more similar compared to individuals with LGD variants in different exons of the same gene (Fig. 3a); 2.2 versus 17.3% difference in the decrease of overall gene dosage (Mann–Whitney U one-tail test $p < 2 \times 10^{-16}$). Moreover, by analyzing GTEx data for each tissue separately, we found that LGD variants in the same exons lead to drastically more similar dosage changes of target genes across tissues (Fig. 3a).

Distinct splicing isoforms often have different functional properties [37, 38]. Therefore, LGD variants may affect phenotypes not only through NMD-induced changes in overall gene dosage, discussed above, but also by altering

the relative expression levels of different splicing isoforms. To specifically analyze changes in the relative expression of splicing isoforms, we next used GTEx variants to quantify how NMD affects the different isoforms of a gene. To compare isoform-specific expression changes in the same gene, we used the angular distance metric between vectors representing dosage changes of each isoform (see Methods). This analysis demonstrated that changes in relative isoform expression were also significantly (~5 fold) more similar for LGD variants in the same exon compared to variants in different exons of the same gene (Fig. 3b); 0.1 versus 0.46 for the average angular distance between isoform expression vectors (Mann–Whitney U one-tail test $p < 2 \times 10^{-16}$). Similar patterns were also observed across human tissues (Fig. 3b). Overall, the analyses of GTEx data demonstrate that both overall changes in gene dosage and changes in the relative expression levels of different splicing isoforms are substantially more similar for truncating mutations in the same exon.

Truncating variants in highly expressed exons should lead to relatively larger NMD-induced decreases in overall gene dosage. To confirm this hypothesis, we used RNA-seq data from GTEx. Specifically, for each exon harboring a truncating variant, we calculated its expression level relative to the expression level of the corresponding gene. We then

explored the relationship between the relative exon expression and the observed NMD-induced decrease in gene expression. The analysis indeed revealed a strong correlation between the relative expression of exons harboring LGDs and the corresponding changes in overall gene dosage (Fig. 3c; Pearson's $R = 0.69$, $p < 2 \times 10^{-16}$; Spearman's $\rho = 0.81$, $p < 2 \times 10^{-16}$; see Methods). NMD-induced dosage changes may mediate the relationship between the relative expression level of target exons and the corresponding phenotypic effect of truncating mutations. To investigate this relationship in detail, we next used the BrainSpan dataset [39], which contains exon-specific expression from human brain tissues. The BrainSpan data allowed us to estimate gene dosage changes resulting from LGD mutations in different exons of ASD-associated genes (see Methods).

It is likely that there is substantial variability across human genes in terms of the sensitivity of intellectual and other ASD phenotypes to gene dosage. Therefore, to quantify the sensitivity of IQ to changes in the expression of specific genes, we used a simple linear dosage model. Specifically, we considered genes with recurrent truncating mutations in SSC, and assumed that for these gene the decrease in probands' IQs is linearly proportional to the NMD-induced decrease in overall gene dosage. We further assumed that each human gene can be characterized by a parameter, which we call phenotype dosage sensitivity (PDS), quantifying the linear relationship between the change in gene dosage compared to wild type and the corresponding changes in a given human phenotype. Numerically, we defined IQ-associated PDS as the average change in IQ resulting from a 10% change in gene dosage. We restricted this analysis to LGD mutations predicted to induce NMD, i.e. we excluded mutations within 50 bp of the last exon junction complex [40], and also assumed the average neurotypical IQ (100) for wild-type (intact) gene dosage. Based on this linear model, for each gene with recurrent truncating ASD mutations, we used predicted gene dosage changes to estimate gene-specific PDS parameters (Supplementary Fig. 11; see Methods). Notably, as expected, PDS values for intellectual phenotypes varied substantially across 24 considered human genes (CV = SD/Mean = 0.57, for NVIQ).

We next used the PDS linear model to explore the relationship between the relative expression values of exons (i.e. the ratio of exon expression to gene expression) harboring LGD mutations and the corresponding decreases in probands' intellectual phenotypes. To account for differences in phenotypic sensitivity to dosage changes across genes, we normalized the observed changes in IQ by the estimated PDS values of affected genes. Normalized in this way, phenotypic effects represent changes in phenotype relative to the predicted effects for 10% decreases in

the dosage of affected genes. This analysis revealed that mutation-induced gene dosage changes are indeed strongly correlated with the normalized phenotypic effects; NVIQ Pearson's $R = 0.63$, permutation test $p = 0.02$ (Fig. 4a and Supplementary Fig. 12). Very weak correlations were obtained for randomly permuted data, i.e. when truncating mutations were randomly re-assigned to different exons in the same gene (average NVIQ Pearson's $R = 0.18$; see Methods). Since the heritability of intelligence is known to substantially increase with age [41], we also investigated how the results depend on the age of probands. When we restricted our analysis to the older half of probands in SSC (i.e. older than the median age of 8.35 years), the strength of the correlations between the predicted dosage changes and normalized phenotypic effects increased further; NVIQ Pearson's $R = 0.75$, average permuted $R = 0.2$, permutation test $p = 0.019$ (Fig. 4b and Supplementary Fig. 13). Overall, these results suggest that, when gene-specific PDS values are taken into account, a significant fraction (30–45%) of the relative phenotypic effects triggered by de novo LGD mutations can be explained by the resulting changes in expression dosage of target genes.

We next evaluated the ability of the linear dosage model to explain the effects of LGD mutations on non-normalized IQs. To that end, for each gene with multiple truncating mutations in different probands, we used the linear regression model to perform leave-one-out predictions for IQ scores, i.e. we used PDS values calculated based on all but one probands with mutations in a gene to estimate IQ values for the left out proband with an LGD mutation in the same gene (Fig. 4c, inset; see Methods). Despite the simplicity of our model, for LGD mutations that trigger NMD, the model median inference error was 11.1 points for NVIQ (Fig. 4c and Supplementary Fig. 14), which is significantly smaller than the median NVIQ difference between probands with LGD mutations in the same gene, 22.0 points (MWU one-tail test $p = 0.014$). The NVIQ inferences based on probands of the same gender had significantly smaller errors compared to inferences based on probands of the opposite gender; same gender NVIQ median error 9.1 points, different gender median error 19.9 points (MWU one-tail test $p = 0.018$). Similar to normalized phenotypic effects (Fig. 4a, b), the inference errors further decreased for older probands; for example, for probands older than 12 years, the median NVIQ inference error was 7.6 points (Fig. 4c and Supplementary Figs. 14 and 15).

Given that relative exon usage varies across neural development [39, 42], we next investigated the relationship between the developmental expression profiles of exons and ASD phenotypes. To that end, we sorted exons from genes harboring LGD mutations [8] into four groups (quartiles) based on their developmental expression bias, which was calculated as the fold-change between the average prenatal
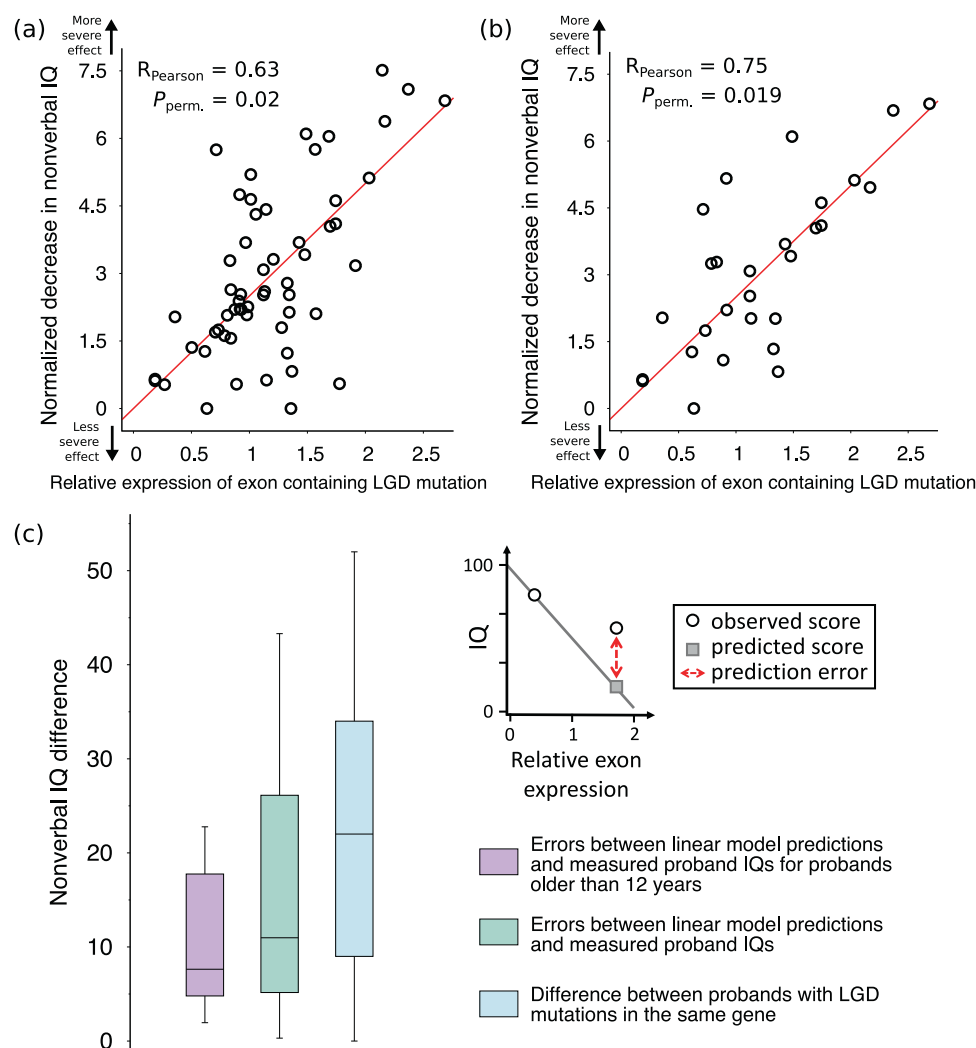
Fig. 4 Relationship between the relative expression of exons harboring LGD mutations and the corresponding decreases in probands' intellectual phenotypes. a Each point corresponds to a proband with a de novo LGD mutation in a gene; only genes with multiple LGD mutations in the SSC cohort were considered. The x-axis represents the relative exon expression level of exons harboring LGD mutations. The y-axis represents the normalized decrease in the affected proband's NVIQ, i.e. the absolute NVIQ decrease divided by the NVIQ phenotype dosage sensitivity (PDS) of the target gene (see Methods). The regression line across all points is shown in red; p values were calculated based on randomly shuffled data (see Methods). **b** Same as **a**, but with the analysis restricted to the older half of SSC probands (i.e. older than the median age 8.35 years). **c** Boxplots represent the distribution of errors in predicting the effects of LGD mutations on NVIQ (see Methods); only genes with multiple LGD mutations in SSC were considered. NVIQ prediction errors are shown for all probands (green), and for probands older than 12 years (purple). For comparison, the average differences in NVIQ scores between pairs of probands with LGD mutations in the same gene are also shown (blue). The ends of each solid box represent the upper and lower quartiles, the horizontal lines inside each box represent the medians, and the whiskers represent the 5th and 95th percentiles. The inset panel illustrates the linear regression used to perform leave-one-out predictions of probands' NVIQs. Round open points represent observed phenotypic scores for probands with distinct LGD mutations in the same gene, the gray square point represents the predicted phenotypic score, and the red dotted line represents the prediction error.

and postnatal exon expression levels (Fig. 5a). We then analyzed the enrichment of LGD mutations in each exon group (see Methods). Compared to exons with no substantial developmental bias, we found significant enrichment of LGD mutations not only in exons with strong prenatal biases (binomial one-tail test $p = 8 \times 10^3$, relative rate = 1.33), but also in exons with postnatal biases ($p = 0.018$, RR = 1.31) (Fig. 5b). To understand the origin of the observed exon developmental biases, we stratified probands into lower (≤ 70) and higher IQ (> 70) cohorts (Fig. 5c). Interestingly, while LGD mutations associated with lower IQs were strongly enriched only in prenatally biased exons (binomial one-tail test $p = 6 \times 10^{-3}$, RR = 1.62), mutations associated with higher IQs were exclusively enriched in postnatally biased exons ($p = 0.05$, RR = 1.27). These results demonstrate that mutations in exons with biases
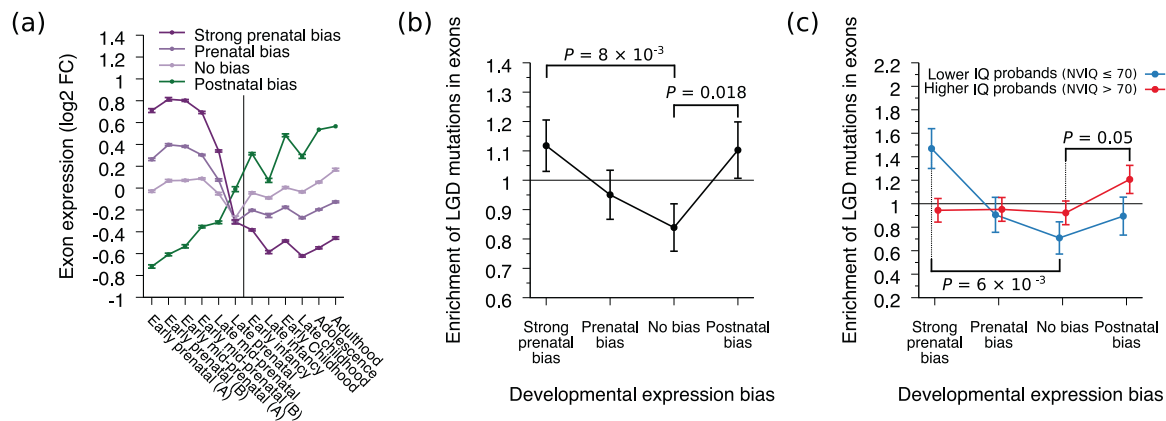
Fig. 5 Relationship between the developmental expression profiles of exons with LGD mutations and intellectual ASD phenotypes. a Developmental expression profiles of exons in genes with de novo LGD mutations in SSC. Exons from all genes harboring LGD mutations were sorted into four groups ("strong prenatal bias", "prenatal bias", "no bias", and "postnatal bias") based on their overall developmental expression bias; the developmental bias was calculated as the $\log_2$ fold-change between the average prenatal and postnatal exon expression levels. Lines represent the average expression profiles of exons in each group, and the x-axis represents 12 periods of human brain development, based on data from the Allen Institute's BrainSpan atlas [45]. The vertical dotted line delineates prenatal and postnatal developmental periods. Error bars represent the SEM. **b, c** Enrichment of LGD mutations across the four exon groups with different developmental biases. The y-axis represents the enrichment (relative rate) of mutations in each exon group; the enrichment was calculated relative to a null model in which LGD mutations were randomized across exons proportionally to the exons' coding sequence lengths (see Methods). Error bars represent the SEM. **b** The overall enrichment of LGD mutations across the four groups of exons with different developmental expression biases. **c** The enrichment of LGD mutations across the four exon groups calculated separately for ASD probands with higher (>70, red) and lower (≤70, blue) nonverbal IQs.

toward prenatal and postnatal expression preferentially contribute to ASD cases with lower and higher IQ phenotypes, respectively. Notably, the exon developmental biases for LGD mutations were not simply driven by expression biases of the corresponding genes, as mutations associated with both higher and lower IQ phenotypes showed enrichment exclusively toward genes with prenatally biased expression (Supplementary Fig. 16).

Although we primarily analyzed in the paper the impact of autism mutations on intellectual phenotypes, changes in the dosage and isoform expression of affected genes may also lead to analogous results for other quantitative ASD phenotypes [24, 43]. Indeed, for LGD mutations predicted to induce NMD, we observed similar patterns for several other key autism phenotypes. Specifically, SSC probands with truncating mutations in the same exon exhibited more similar adaptive behavior abilities compared to probands with mutations in the same gene (Fig. 6a, left set of bars, and Supplementary Fig. 17); Vineland Adaptive Behavior Scales (VABS) [44] composite standard score difference of 4.7 versus 12.1 points (Mann–Whitney U one-tail test $p = 0.017$). In contrast, VABS score differences between probands with truncating mutations in the same gene were not significantly different than for randomly paired probands (Fig. 6a and Supplementary Fig. 17); 12.1 versus 13.7 points (MWU one-tail test $p = 0.23$). Probands with truncating mutations in the same exon also displayed more similar fine motor skills; in the Purdue Pegboard Test, 1.2 versus 3.0 for the average difference in normalized tasks

completed with both hands (MWU one-tail test $p = 0.02$; Supplementary Fig. 18; see Methods). Coordination scores in the Social Responsiveness Scale questionnaire were also more similar in probands with LGD mutations in the same exon compared to probands with mutations in the same gene; 0.6 versus 1.1 for the average difference in normalized response (MWU one-tail test $p = 0.05$; Supplementary Fig. 19).

Finally, we sought to validate the observed phenotypic patterns using an independent ASD cohort. To that end, we analyzed an independently collected dataset from the ongoing Simons VIP project [29]. The analyzed VIP dataset contained genetic information and VABS phenotypic scores for 41 individuals with de novo LGD mutations in 12 genes. Reassuringly, in agreement with our findings in SSC, probands from the VIP cohort with truncating de novo mutations in the same exon also exhibited strikingly more similar VABS phenotypic scores compared to probands with mutations in the same gene (Fig. 6a, right set of bars and Supplementary Fig. 20); VABS composite standard score difference 6.0 for LGDs in the same exon versus 12.4 for LGDs in the same gene (Mann–Whitney U one-tail test $p = 0.014$). Similar to the SSC cohort, LGD mutations in neighboring exons did not result in more similar behavior phenotypes; VABS composite standard score average difference 13.6 points (MWU one-tail test $p = 0.6$). The fraction of truncated proteins also did not show significant correlation with the VABS scores of affected probands (Pearson's $R = -0.08$, $p = 0.7$). Using VABS scores from
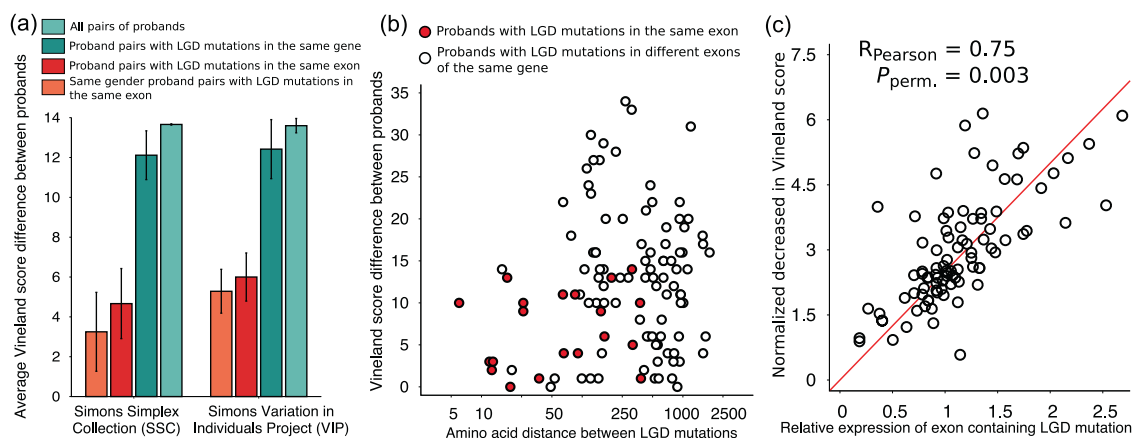
Fig. 6 Validation of the observed phenotypic patterns in independent cohorts using Vineland Adaptive Behavior Scales (VABS) scores. a Average VABS score differences between pairs of probands based on data from the SSC cohort (left set of bars) and the VIP cohort (right set of bars). Each bar shows the average difference in VABS scores between pairs of probands in different groups. In the SSC and VIP bar sets, from right to left, the bars represent differences between all pairs of probands in each cohort (light green), between pairs of probands with LGD mutations in the same gene (dark green), between probands with LGD mutations in the same exon (red), and between pairs of probands of the same gender with LGD mutations in the same exon (orange). Error bars represent the SEM. **b** Amino acid distance between the sites of LGD mutations in the same protein versus probands' differences in VABS score. Each point corresponds to a pair of probands, for individuals from either SSC or VIP, with LGD mutations in the same gene. The x-axis represents the amino acid distance between the protein sites of LGD mutations, and the y-axis

represents the difference between the corresponding probands' VABS scores. Red points represent proband pairs with LGD mutations in the same exon, and white points represent proband pairs with LGD mutations in different exons of the same gene. **c** Relationship between the relative expression of exons harboring LGD mutations and the corresponding decrease in probands' normalized VABS scores. Each point corresponds to a proband with an LGD mutation in a gene; only genes with multiple LGD mutations were considered. The x-axis represents the relative expression (exon expression level divided by overall gene expression level) of exons harboring LGD mutations. The y-axis represents normalized decreases in VABS scores of affected probands, i.e. the absolute VABS score decrease divided by the VABS phenotypic dosage sensitivity (PDS) of the target gene. The regression line across all points is shown in red; p values were calculated based on randomly shuffled data (see Methods). The analysis was restricted to de novo LGD mutations predicted to trigger NMD, i.e. mutations located more than 50 bp upstream from the last exon junction.

both SSC and VIP, we next investigated whether, analogous to the IQ phenotypes (Fig. 3a), the similarity of VABS scores is primarily due to the occurrence of LGD mutations in the same exon, rather than simply the proximity of mutations in the corresponding protein sequence. Indeed, LGD mutations in the same exon often resulted in similar adaptive behavior abilities even when the corresponding mutations were separated by hundreds of amino acids (Fig. 6b, red points, and Supplementary Fig. 21). By comparing mutations in the same exon to mutations at similar amino acid distances in the same protein but not necessarily the same exon, we confirmed that probands with mutations in the same exon were significantly more phenotypically similar (permutation test $p = 3 \times 10^{-4}$; Supplementary Fig. 22; see Methods). When we applied the developed linear dosage model to account for the sensitivity of VABS to changes in the dosage of different genes (i.e. gene-specific PDS values), we found substantial correlations between the relative expression of exons harboring LGD mutations and the normalized VABS phenotypes of the affected probands (Pearson $R = 0.75$, permutation test $p = 0.003$; Fig. 6c and Supplementary Fig. 23). Overall, these results confirm the generality of the phenotypic patterns observed in the SSC cohort.

Discussion

Previous studies explored phenotypic similarity in syndromic forms of ASD due to mutations in specific genes [45–49]. Nevertheless, across a large collection of contributing genes, the nature of the substantial phenotypic heterogeneity in ASD is not well understood. Interestingly, the diversity of intellectual and other important autism phenotypes resulting from de novo LGD mutations in the same genes is usually only slightly (~10%) smaller than the phenotypic heterogeneity across entire ASD cohorts (Figs. 1 and 6a). The presented results suggest that truncating mutations usually result in a range of relatively mild NMD-induced changes in gene dosage, on average decreasing gene expression by ~15–30% (Supplementary Fig. 24; see Methods). Our study further suggests a hierarchy of biological mechanisms contributing to phenotypic heterogeneity in simplex ASD cases that are triggered by LGD mutations in different genes and within the same gene.

Across LGD mutations in different probands, there is a significant but small correlation between a target gene's brain expression level and the resulting intellectual phenotypes ($R^2 = 0.02$ for NVIQ, $p = 0.03$). This correlation is small, at least in part, due to the significant variability of

expression levels of different exons in a given gene. Indeed, intellectual phenotypes correlate significantly better with the relative expression level of exons harboring LGD mutations ($R^2 = 0.10$, $p = 0.011$). In addition to effects associated with different expression levels of exons, there is also substantial variability in the sensitivity of each specific phenotype to changes in the expression dosage of the target gene. When we accounted for different dosage sensitivities using gene-specific PDS values, the correlation between predicted dosage changes and normalized phenotypic effects became substantial ($R^2 = 0.4$, $p = 0.02$, Figs. 4a and 6c). As the heritability of IQ phenotypes usually increases with age, we observed even stronger dosage–phenotype correlations for older probands ($R^2 = 0.56$, $p = 0.019$, Fig. 4b). Furthermore, even perturbations leading to similar dosage changes in the same target gene may result in diverse phenotypes in cases where splicing isoforms with different functional properties are truncated. However, when exactly the same sets of isoforms are perturbed, as for LGD mutations in the same exon, the resulting phenotypes, even in unrelated ASD probands, become especially similar (Figs. 1 and 6a). For LGD mutations affecting intellectual phenotypes, we found that same exon membership accounts for a larger fraction of phenotypic variance than multiple other genomic features, including expression, evolutionary conservation, pathway membership, and domain truncation (see Methods). There are certainly many deviations from the aforementioned average patterns for specific genes and truncating mutations. For example, truncated proteins that escape NMD may lead to partial buffering due to remaining protein activity or to more damaging effects due to dominant negative interactions. Nevertheless, our results demonstrate that for de novo LGD mutations in ASD, exons, rather than genes, usually represent a unit of effective phenotypic impact.

Our results also suggest that ASD phenotypes induced by LGD mutations may be characterized by a simple linear model quantifying the sensitivity of a given phenotype to changes in gene dosage. We observe that PDS values for the same phenotype vary substantially across genes (Supplementary Fig. 11), and that PDS differences are a major source of phenotypic variability. PDS values for the same gene also vary across phenotypes (for example, the correlation between PDS values for IQ and VABS across 24 genes was $R^2 = 0.37$, $p = 0.001$), which suggests that PDS values are likely to be specific to each phenotype–gene pair. Although we evaluated PDS parameters using NMD-induced dosage changes, it may be possible to infer these parameters based on other mechanisms of dosage change, such as regulatory mutations. As genetic and phenotypic data accumulate, it will be interesting to estimate gene-specific PDS values for multiple phenotypes and for a large number of ASD risk genes. Due to analogous patterns of gene expression changes across tissues (Fig. 3), it may be also possible to estimate PDS parameters for other genetic disorders and phenotypes. We note in this respect that gene–dosage relationships have been recently characterized for quantitative yeast fitness phenotypes in different environmental conditions [50].

In the present study, we specifically focused on simplex cases of ASD, in which de novo LGD mutations are highly penetrant and where the contribution of genetic background is naturally minimized. Nevertheless, differences in genetic background and environment represent other important sources of phenotypic variability [22, 51, 52]. In more diverse ASD cohorts, individuals with LGD mutations in the same exon will likely display greater phenotypic heterogeneity. For example, the Simons VIP identified substantial phenotypic variability associated with specific genetic insults in general ASD cohorts [29, 53–55]. We also observed significantly larger phenotypic variability for probands from sequenced family trios, i.e. families without unaffected siblings (Supplementary Fig. 25). For these probands, the enrichment of de novo LGD mutations is substantially lower and the contribution from genetic background is likely to be larger [56], resulting in more pronounced phenotypic diversity.

Our study may have important implications for precision medicine [51, 57, 58]. The presented results suggest that relatively mild decreases in affected gene dosage may account for a substantial fraction of the adverse phenotypic consequences in ASD. Thus, from a therapeutic perspective, compensatory expression of intact alleles, as was recently demonstrated in mouse models of autism [59–61] and other diseases [62], may provide an approach for alleviating phenotypic effects for at least a fraction of ASD cases. From a prognostic perspective, our results indicate that by sequencing and phenotyping sufficiently large patient cohorts, it may be possible to understand likely phenotypic consequences triggered by LGD mutations in specific exons. Furthermore, because we observe consistent patterns of expression changes across multiple human tissues, similar analyses may be extended to other disorders affected by highly penetrant truncating mutations.

Compliance with ethical standards

Conflict of interest The authors declare that they have no conflict of interest.

References

1. Gilman SR, Chang J, Xu B, Bawa TS, Gogos JA, Karayiorgou M, et al. Diverse types of genetic variation converge on functional gene networks involved in schizophrenia. Nat Neurosci. 2012;15:1723–8.

2. Ayalew M, Le-Niculescu H, Levey DF, Jain N, Changala B, Patel SD, et al. Convergent functional genomics of schizophrenia: from comprehensive understanding to genetic risk prediction. Mol Psychiatry. 2012;17:887–905.

3. Fromer M, Pocklington AJ, Kavanagh DH, Williams HJ, Dwyer S, Gormley P, et al. De novo mutations in schizophrenia implicate synaptic networks. Nature. 2014;506:179–84.

4. Parikshak NN, Gandal MJ, Geschwind DH. Systems biology and gene networks in neurodevelopmental and neurodegenerative disorders. Nat Rev Genet. 2015;16:441–58.

5. Chang J, Gilman SR, Chiang AH, Sanders SJ, Vitkup D. Genotype to phenotype relationships in autism spectrum disorders. Nat Neurosci. 2015;18:191–8.

6. Gilman SR, Iossifov I, Levy D, Ronemus M, Wigler M, Vitkup D. Rare de novo variants associated with autism implicate a large functional network of genes involved in formation and function of synapses. Neuron. 2011;70:898–907.

7. Sanders SJ, Ercan-Sencicek AG, Hus V, Luo R, Murtha MT, Moreno-De-Luca D, et al. Multiple recurrent de novo CNVs, including duplications of the 7q11.23 Williams syndrome region, are strongly associated with autism. Neuron. 2011;70:863–85.

8. Iossifov I, O'Roak BJ, Sanders SJ, Ronemus M, Krumm N, Levy D, et al. The contribution of de novo coding mutations to autism spectrum disorder. Nature. 2014;515:216–21.

9. Satterstrom FK, Kosmicki JA, Wang J, Breen MS, De Rubeis S, An J-Y, et al. Large-Scale exome sequencing study implicates both developmental and functional changes in the neurobiology of autism. Cell. 2020;180:568–.e23.

10. O'Roak BJ, Vives L, Girirajan S, Karakoc E, Krumm N, Coe BP, et al. Sporadic autism exomes reveal a highly interconnected protein network of de novo mutations. Nature. 2012;485:246–50.

11. American Psychiatric Association (DSM-5 Task Force). Diagnostic and Statistical Manual of Mental Disorders: DSM-5. 5th ed. Washington, DC: American Psychiatric Association; 2013.

12. Krumm N, O'Roak BJ, Shendure J, Eichler EE. A de novo convergence of autism genetics and molecular neuroscience. Trends Neurosci. 2014;37:95–105.

13. Ronemus M, Iossifov I, Levy D, Wigler M. The role of de novo mutations in the genetics of autism spectrum disorders. Nat Rev Genet. 2014;15:133–41.

14. de la Torre-Ubieta L, Won H, Stein JL, Geschwind DH. Advancing the understanding of autism disease mechanisms through genetics. Nat Med. 2016;22:345–61.

15. Jeste SS, Geschwind DH. Disentangling the heterogeneity of autism spectrum disorder through genetic findings. Nat Rev Neurol. 2014;10:74–81.

16. Talkowski ME, Minikel EV, Gusella JF. Autism spectrum disorder genetics: diverse genes with diverse clinical outcomes. Harv Rev Psychiatry. 2014;22:65–75.

17. Gaugler T, Klei L, Sanders SJ, Bodea CA, Goldberg AP, Lee AB, et al. Most genetic risk for autism resides with common variation. Nat Genet. 2014;46:881–5.

18. Gratten J, Wray NR, Keller MC, Visscher PM. Large-scale genomics unveils the genetic architecture of psychiatric disorders. Nat Neurosci. 2014;17:782–90.

19. Anney R, Klei L, Pinto D, Almeida J, Bacchelli E, Baird G, et al. Individual common variants exert weak effects on the risk for autism spectrum disorders. Hum Mol Genet. 2012;21:4781–92.

20. Krumm N, Turner TN, Baker C, Vives L, Mohajeri K, Witherspoon K, et al. Excess of rare, inherited truncating mutations in autism. Nat Genet. 2015;47:582–8.

21. Turner TN, Coe BP, Dickel DE, Hoekzema K, Nelson BJ, Zody MC, et al. Genomic patterns of de novo mutation in simplex autism. Cell. 2017;171:710–.e712.

22. Robinson EB, Samocha KE, Kosmicki JA, McGrath L, Neale BM, Perlis RH, et al. Autism spectrum disorder severity reflects the average contribution of de novo and familial influences. Proc Natl Acad Sci. 2014;111:15161–5.

23. Levy D, Ronemus M, Yamrom B, Lee YH, Leotta A, Kendall J, et al. Rare de novo and transmitted copy-number variation in autistic spectrum disorders. Neuron. 2011;70:886–97.

24. Buja A, Volfovsky N, Krieger AM, Lord C, Lash AE, Wigler M, et al. Damaging de novo mutations diminish motor skills in children on the autism spectrum. Proc Natl Acad Sci. 2018;115: E1859–66.

25. Taylor LJ, Maybery MT, Wray J, Ravine D, Hunt A, Whitehouse AJO. Are there differences in the behavioural phenotypes of Autism Spectrum Disorder probands from simplex and multiplex families? Res Autism Spectr Disord. 2015;11:56–62.

26. Dissanayake C, Searles J, Barbaro J, Sadka N, Lawson LP. Cognitive and behavioral differences in toddlers with autism spectrum disorder from multiplex and simplex families. Autism Res. 2019;12:682–93.

27. Berends D, Dissanayake C, Lawson LP. Differences in cognition and behaviour in multiplex and simplex autism: does prior experience raising a child with autism matter? J Autism Developmental Disord. 2019;49:3401–11.

28. Fischbach GD, Lord C. The Simons Simplex Collection: a resource for identification of autism genetic risk factors. Neuron. 2010;68:192–5.

29. Simons VIP. Consortium. Simons Variation in Individuals Project (Simons VIP): a genetics-first approach to studying autism spectrum and related neurodevelopmental disorders. Neuron. 2012;73:1063–7.

30. Fombonne E. Epidemiology of pervasive developmental disorders. Pediatr Res. 2009;65:591–8.

31. Robinson EB, Lichtenstein P, Anckarsäter H, Happé F, Ronald A. Examining and interpreting the female protective effect against autistic behavior. Proc Natl Acad Sci. 2013;110:5258–62.

32. El-Gebali S, Mistry J, Bateman A, Eddy SR, Luciani A, Potter SC, et al. The Pfam protein families database in 2019. Nucleic Acids Res. 2018;47:D427–32.

33. Chang YF, Imam JS, Wilkinson MF. The nonsense-mediated decay RNA surveillance pathway. Annu Rev Biochem. 2007;76:51–74.

34. GTEx Consortium. Human genomics. The Genotype-Tissue Expression (GTEx) pilot analysis: multitissue gene regulation in humans. Science. 2015;348:648–60.

35. Mele M, Ferreira PG, Reverter F, DeLuca DS, Monlong J, Sammeth M, et al. Human genomics. The human transcriptome across tissues and individuals. Science. 2015;348:660–5.

36. Rivas MA, Pirinen M, Conrad DF, Lek M, Tsang EK, Karczewski KJ, et al. Human genomics. Effect of predicted protein-truncating genetic variants on the human transcriptome. Science. 2015;348:666–9.

37. Keren H, Lev-Maor G, Ast G. Alternative splicing and evolution: diversification, exon definition and function. Nat Rev Genet. 2010;11:345–55.

38. Yang X, Coulombe-Huntington J, Kang S, Sheynkman GM, Hao T, Richardson A, et al. Widespread expansion of protein interaction capabilities by alternative splicing. Cell. 2016;164:805–17.

39. Kang HJ, Kawasawa YI, Cheng F, Zhu Y, Xu X, Li M, et al. Spatio-temporal transcriptome of the human brain. Nature. 2011;478:483–9.

40. Nagy E, Maquat LE. A rule for termination-codon position within intron-containing genes: when nonsense affects RNA abundance. Trends Biochemical Sci. 1998;23:198–9.

41. Haworth CMA, Wright MJ, Luciano M, Martin NG, de Geus EJC, van Beijsterveldt CEM, et al. The heritability of general cognitive ability increases linearly from childhood to young adulthood. Mol Psychiatry. 2009;15:1112–20.

42. Weyn-Vanhentenryck SM, Feng H, Ustianenko D, Duffie R, Yan Q, Jacko M, et al. Precise temporal regulation of alternative splicing during neural development. Nat Commun. 2018;9:2189.

43. Bishop SL, Farmer C, Bal V, Robinson E, Willsey AJ, Werling DM, et al. Identification of developmental and behavioral markers associated with genetic abnormalities in autism spectrum disorder. Am J Psychiatry. 2017;174:576–85.

44. Zerbino DR, Achuthan P, Akanni W, Amode MR, Barrell D, Bhai J, et al. Ensembl 2018. Nucleic Acids Res. 2017;46:D754–61.

45. Sztainberg Y, Zoghbi HY. Lessons learned from studying syndromic autism spectrum disorders. Nat Neurosci. 2016;19:1408–17.

46. Bernier R, Golzio C, Xiong B, Stessman HA, Coe BP, Penn O, et al. Disruptive CHD8 mutations define a subtype of autism early in development. Cell. 2014;158:263–76.

47. Helsmoortel C, Vulto-van Silfhout AT, Coe BP, Vandeweyer G, Rooms L, van den Ende J, et al. A SWI/SNF-related autism syndrome caused by de novo mutations in ADNP. Nat Genet. 2014;46:380–4.

48. Van Bon B, Coe B, Bernier R, Green C, Gerdts J, Witherspoon K, et al. Disruptive de novo mutations of DYRK1A lead to a syndromic form of autism and ID. Mol Psychiatry. 2016;21:126–32.

49. Ben-Shalom R, Keeshen CM, Berrios KN, An JY, Sanders SJ, Bender KJ. Opposing effects on NaV1.2 function underlie differences between SCN2A variants observed in individuals with autism spectrum disorder or infantile seizures. Biol Psychiatry. 2017;82:224–32.

50. Keren L, Hausser J, Lotan-Pompan M, Vainberg Slutskin I, Alisar H, Kaminski S, et al. Massively parallel interrogation of the effects of gene expression levels on fitness. Cell. 2016;166:1282–.e1218.

51. Gandal MJ, Leppa V, Won H, Parikshak NN, Geschwind DH. The road to precision psychiatry: translating genetics into disease mechanisms. Nat Neurosci. 2016;19:1397–407.

52. Robinson EB, St Pourcain B, Anttila V, Kosmicki JA, Bulik-Sullivan B, Grove J, et al. Genetic risk for autism spectrum disorders and neuropsychiatric variation in the general population. Nat Genet. 2016;48:552–5.

53. Qureshi AY, Mueller S, Snyder AZ, Mukherjee P, Berman JI, Roberts TP, et al. Opposing brain differences in 16p11. 2 deletion and duplication carriers. J Neurosci. 2014;34:11199–211.

54. Hanson E, Bernier R, Porche K, Jackson FI, Goin-Kochel RP, Snyder LG, et al. The cognitive and behavioral phenotype of the 16p11.2 deletion in a clinically ascertained population. Biol Psychiatry. 2015;77:785–93.

55. D'Angelo D, Lebon S, Chen Q, Martin-Brevet S, Snyder LG, Hippolyte L, et al. Defining the effect of the 16p11.2 duplication on cognition, behavior, and medical comorbidities. JAMA Psychiatry. 2016;73:20–30.

56. Zhao X, Leotta A, Kustanovich V, Lajonchere C, Geschwind DH, Law K, et al. A unified genetic theory for sporadic and inherited autism. Proc Natl Acad Sci. 2007;104:12831–6.

57. Collins FS, Varmus H. A new initiative on precision medicine. N Engl J Med. 2015;372:793–5.

58. Geschwind DH, State MW. Gene hunting in autism spectrum disorder: on the path to precision medicine. Lancet Neurol. 2015;14:1109–20.

59. Guy J, Gan J, Selfridge J, Cobb S, Bird A. Reversal of neurological defects in a mouse model of Rett syndrome. Science. 2007;315:1143–7.

60. Mei Y, Monteiro P, Zhou Y, Kim J-A, Gao X, Fu Z, et al. Adult restoration of Shank3 expression rescues selective autistic-like phenotypes. Nature. 2016;530:481–4.

61. Ehninger D, Han S, Shilyansky C, Zhou Y, Li W, Kwiatkowski DJ, et al. Reversal of learning deficits in a $Tsc2^{+/-}$ mouse model of tuberous sclerosis. Nat Med. 2008;14:843–8.

62. Matharu N, Rattanasopha S, Tamura S, Maliskova L, Wang Y, Bernard A, et al. CRISPR-mediated activation of a promoter or enhancer rescues obesity caused by haploinsufficiency. Science. 2019;363:eaau0629.